Rooted Tree Optimization for Backstepping Power Control of DFIG Wind Turbine: dSPACE Implementation

Badre BOSSOUFI (badre.bossoufi@usmba.ac.ma)
Sidi Mohamed Ben Abdellah University
Mohammed KARIM
Sidi Mohamed Ben Abdellah University
Mohammed Taoussi
Sidi Mohamed Ben Abdellah University
Hala Alami Aroussi
Mohamed I University
Olivier Deblecker
University of Mons
Saad Motahhir
Sidi Mohamed Ben Abdellah University
Anand Nayyar
Duy Tan University
Mehedi Masud
Taif University
Manale Boderbala
Sidi Mohamed Ben Abdellah University

Research Article

Keywords: DFIG, Backstepping Control, Adaptative control, Matlab/Simulink, Wind Turbine, dSPACE

Posted Date: November 24th, 2020

DOI: https://doi.org/10.21203/rs.3.rs-107889/v1

Rooted Tree Optimization for Backstepping Power Control of DFIG Wind Turbine: dSPACE Implementation

Badre Bossoufi[1], Mohammed Karim[1], Mohammed Taoussi[1], Hala Alami-Aroussi[2], Manale Bouderbala[1], Olivier Deblecker[3], Saad Motahhir[4], Anand Nayyar[5], Mehedi Masud[6]

[1]LIMAS Laboratory, Faculty of Sciences, Sidi Mohamed Ben Abdellah University, Fez, Morocco
[2] LGEM Laboratory, Higher School of Technology, Mohammed First University, Oujda, Morocco.
[3] EPEU unit, Polytech of Mons, Mons, Belgium.
[4] Engineering, Systems and Applications Laboratory, Sidi Mohamed Ben Abdellah University, Fez, Morocco
[5] Graduate School, Faculty of Information Technology, Duy Tan University, Da Nang 550000, Viet Nam
[6] Department of Computer Science, College of Computers and Information Technology, Taif University, Taif, Saudi Arabia

Badre.bossoufi@usmba.ac.ma

***Abstract*— This work is devoted to a new contribution to the field of optimization and control of a wind energy conversion system (WECS). A Rooted Tree Optimisation (RTO) will be applied to the non-linear adaptive Backstepping technique to improve its robustness and performance. The non-linear Backstepping control was carried out to control the powers of the doubly-fed induction generator (DFIG) connected to the electrical network by two converters (network side and machine side). Initially, a review of the wind power system was presented. Then, an exhaustive explanation of the Backstepping technique based on the Lyapunov stability and the optimization method was reported. Subsequently, a validation on the Matlab & Simulink environment was carried out to test the performance and robustness of the proposed model. The last part of this work was dedicated to the experiment of the Backstepping adaptive algorithm on a test bench using the dSPACE-DS1104 card, to prove the performance of the system. The results obtained of this work either by follow-up or robustness tests or by experimental validation show a great improvement in terms of performance compared to other control techniques.**

***Index Terms*— DFIG, Backstepping Control, Adaptative control, Matlab/Simulink, Wind Turbine, dSPACE.**

1. Introduction

Nowadays, renewable energies become the most coveted energies since they ensure autonomy for all nations [1]. Created from inexhaustible resources, they need no storage. Their utilization guarantees the continuity of the production without worrying about fluctuations in the prices of raw material in the international energy markets [2].

Sustainable power sources are the most reasonable way to improve decentralized energy supplying. These resources are especially significant for certain arising nations but also developed countries. Indeed, the utilization of this kind of energies makes it conceivable, to enhance the common assets of the regions by creating new industries, transport, and urbanization, etc. It controls the exploitation and reduces the consumption of fuel [3]. Besides, it diminishes the cost of energy production contrasted with classical energies.

These days, renewable sources provide an impressive potential for a financial, modern, and social turn of events. The fast development of the global environmentally friendly power markets makes different project openings attached to every sector. The rivalry is all-inclusive. Moreover, it will quicken the portion of sustainable power sources in the worldwide energy mix at an undeniably serious cost and make new businesses.

The International Energy Agency forecasts that renewable energies should cover, in 2040, 58% of the supplies in electricity, 22% for the creation of inexhaustible warmth and cold and 20% for transport if we want to keep the temperature on the surface of the globe under 2 °C. Indeed, Sustainable power sources will close to 60% of the emerged installation till 2040. Between 2016 and 2040, over 4,000 GW must be operating that represent four times the thermal capacity manufactured in the same period. Numerous reasons endorse this enhancement: the decrease of costs, the dispersion of innovations on a worldwide scale, the economic and international pressures associated with the massive uses of hydrocarbons, the determination to respect the commitments of the Paris agreement…

The goals of this work are [4]:

- The decrease in the expense related to the production of electrical energy by solar and wind power plants. Improving the quality of electrical energy supplied by solar and wind power plants.

- The proposal of logical answers for the implementation of inexhaustible sources in smart grids that require reliable production systems.

The achievement of these objectives will promote the enhancement of electrical energy quality produced by sustainable sources [5]. This improvement in production will impact the selling price of this energy. Nevertheless, we have to bring out the important constituent that assures this progress, which are the control strategies [6].

The reduction in the cost of electrical energy presupposes, among other things:

- The rise of reliability and robustness for wind power plants.
- The manufacture of lighter wind turbines (WTs) with high performance.
- The increase in energy efficiency.
- The robustness of the designed control algorithms.

The decentralized energy sources have some drawbacks such as no voltage adjustment, no frequency regulation, no possibility of operating in islanding, etc.). Indeed, energy production from renewable energy sources is difficult to predict and fluctuates widely. So, the integration of decentralized units into the electrical grid will certainly cause some problems as mentioned previously [7].

This document sets a target which is the application of a non-linear adaptive Backstepping command in real-time on a WECS-DFIG, controlled by power converters (grid and generator sides). Moreover, the main objective is to command the wind system via the DS1104 R&D card under variable wind reference. In this work, our contribution will be as follows:

- Ensure and optimize the operation of the wind system with a non-linear model of the system using a non-linear control technique.
- Implement and validate experimentally our model in a Benchmark based on a DFIG of 1,5KW and a dSPACE DS1104 card.

This paper is divided into five sections: the first section gives a summary of some recent studies on control strategies in the field of wind energy. *Section II* explains the modeling of some parts of the wind energy conversion system adopted. The development of the Backstepping technique that is based on the Lyapunov stability will be detailed in *Section III*. Thereafter, Section *V* will be dedicated to the validation of the Backstepping algorithm on a testbench based on a dSPACE card, including a discussion of the results found. At the end, a conclusion of this study is exposed to summarize and show the efficiency of the Backstepping control.

2. Literature review

Based on several works in the literature that develop classical techniques: Backstepping control, sliding mode control (SMC), field-oriented control, and predictive control, we will develop a new robust and optimal control strategy and overcome the disadvantages of these types of control. In this section we present some examples:

Zhe Zhang et al. (2014) [8] presents a work based on the application of the DTC command (based on vector SVM) for a PMSG-based wind system, he combined this command with an observer in the sliding mode which uses a relatively low sampling frequency, to estimate the position of the rotor and the stator flux connection.

Beltran et al. (2012) [9] presents in his work the application of the MPPT command and the sliding mode control for a wind power system based on DFIG. His work aims to control the desired electromagnetic torque using the control of the currents. Also, the use of estimates to define the references that causes certain inaccuracies leading mainly to a non-optimal power extraction.

BoYang et al. (2017) [10] treats the application of the sliding mode control strategy (SMC) on the DFIG. The results obtained are good but present several problems (chattering phenomenon).

Benbouzid et al. (2010) [11] presents in his work a control that leads to the production of electricity under variable speed for wind turbine systems. These systems have two operating zones which depend on the wind turbine tip speed ratio. A high order sliding mode strategy is then suggested to guarantee stability in the two operating zones and execute the optimal.

According to this brief study, the majority of control algorithms, either for a DFIG-based or PMSG-based wind system, encounter problems in terms of robustness and also in real-time implantation. Our contribution in this work is to confirm the performance of an adaptive model using the implementation and validation on a test bench based on a dSPACE card which is rarely discussed.

3. Wind-power system model

The development of Backstepping control for the wind system requires a specific model (non-linear) of the machine. This is why the analytical model of the doubly-fed induction generator is essential. The equivalent model adopted must be close to reality and not linear to facilitate implementation [12].
The structure of the wind power system is illustrated in Fig. 1. [5]

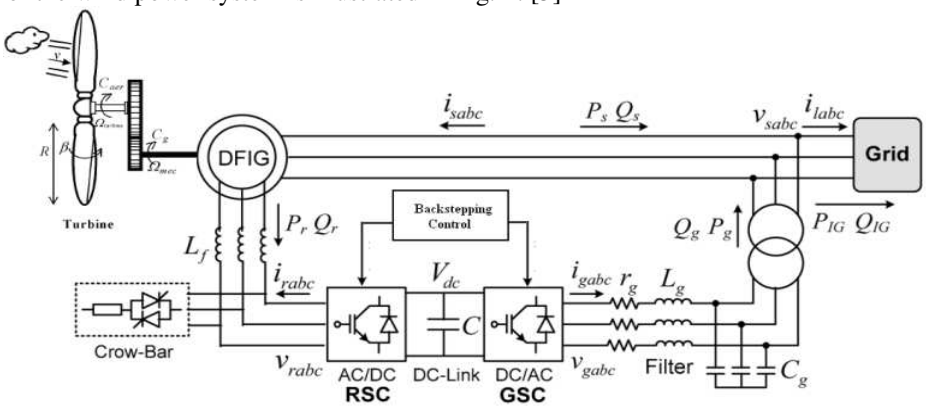

Fig.1. Wind power system structure
The goal of this part is to model the WECS-DFIG: modelling of the kinetic (Turbine), mechanical (Shaft and Gearbox), and electrical (Generator, Converters, DC-link, filter..) parts.
The structure of the whole system is displayed in the figure above.

A. Wind Turbine model

The turbine model is deduced from the following equations [1]:

$$P_{incident} = \frac{1}{2}.\rho.A.v^3 \tag{1}$$

$$P_{extracted} = \frac{1}{2}.\rho.A.C_p(\lambda,\beta).v^3 \tag{2}$$

With $\lambda = \frac{\Omega_t.R}{v}$ (3)

$$J = \frac{J_{tur}}{G^2} + J_g \tag{4}$$

$$J\frac{d\Omega_{mec}}{dt} = C_{mec} = C_{ar} - C_{em} - f.\Omega_{mec} \tag{5}$$

B. Doubly Fed Induction Generator-Model:

Many researchers represent the DFIG model in the reference dq by four types of equations [13, 18]:
1) Electrical equations:
The voltages in the reference frame dq yields:

$$\begin{cases} V_{sd} = R_s.I_{sd} + \frac{d\phi_{sd}}{dt} - \omega_s.\phi_{sq} \\ V_{sq} = R_s.I_{sq} + \frac{d\phi_{sq}}{dt} + \omega_s.\phi_{sd} \\ V_{rd} = R_r.I_{rd} + \frac{d\phi_{rd}}{dt} - \omega_r.\phi_{rq} \\ V_{rq} = R_r.I_{rq} + \frac{d\phi_{rq}}{dt} + \omega_r.\phi_{rd} \end{cases} \tag{6}$$

2) Flux equations:
The fluxes (stator & rotor) are connected to currents (stator & rotor) by the expressions below:

$$\omega_r = \omega_s - p.\Omega$$

$$\begin{cases} \varphi_{ds} = L_s.i_{ds} + M.i_{dr} \\ \varphi_{qs} = L_s.i_{qs} + M.i_{qr} \\ \varphi_{dr} = L_r.i_{dr} + M.i_{ds} \\ \varphi_{qr} = L_r.i_{qr} + M.i_{qs} \end{cases} \tag{7}$$

$$L_s = l_s - M_s, \qquad L_r = l_r - M_r$$

3) Electromagnetic torque:
The electromagnetic torque is expressed as a function of the stator flux and stator current by[1]:

$$C_{em} = p(\phi_{ds} i_{qs} - \phi_{qs} i_{ds}) \tag{8}$$

4) Active and reactive powers:

The stator and rotor powers (active & reactive) of the DFIG are written as [1]:

$$\begin{cases} P_s = v_{ds}.i_{ds} + v_{qs}.i_{qs} \\ Q_s = v_{qs}.i_{ds} - v_{ds}.i_{qs} \\ P_r = v_{dr}.i_{dr} + v_{qr}.i_{qr} \\ Q_r = v_{qr}.i_{dr} - v_{dr}.i_{qr} \end{cases} \tag{9}$$

4. Backstepping control technique

A. Rotor Side Converter Control

In this part, we propose a control model which is the non-linear Backstepping technique (based on the Lyapunov function) adaptive with a machine parameter estimator [1, 14].

The rotor side control aims to ensure the stability of the active and reactive powers. First, we define the errors, such as:

$$e_{P_s} = P_{s\_ref} - P_s \tag{10}$$

$$e_{Q_s} = Q_{s\_ref} - Q_s \tag{11}$$

Then, we express the Lyapunov function as [13-14]:

$$V_1 = \frac{1}{2} e_{P_s}^2 \tag{12}$$

$$V_2 = \frac{1}{2}\left(e_{P_s}^2 + e_{Q_s}^2\right) \tag{13}$$

To make sure that the stability of the system is realized, it is necessary to guarantee the negativity of the derivative of Lyapunov functions (V_1 and V_2). For this, we introduce a positive constant in the derivative of (V_1 and V_2):

$$\dot{V}_1 = -k_{Ps} e_{Ps}^2 \leq 0 \tag{14}$$

$$\dot{V}_2 = -K_{Vdc} e_{Vdc} - K_{Ps} e_{Pq} - K_{Qs} e_{Qs} \leq 0 \tag{15}$$

After calculation, we get the vectors:

$$\begin{cases} v_{rd} = \frac{1}{v_{sd} M}\begin{pmatrix} \left(\frac{2\sigma L_s L_r}{3}\right)\left(K_{Ps} e_{Ps} + \dot{P}_{s-ref} - \omega_s Q_s\right) \\ \frac{2}{3}(R_s L_r + R_r L_s) P_s + (R_r + \omega_r L_r)\left(v_{sd}\varphi_{sd} + v_{sq}\varphi_{sq}\right) + L_r V_s^2 \end{pmatrix} \\ v_{rq} = -\frac{1}{v_{sd} M}\begin{pmatrix} \left(\frac{2\sigma L_s L_r}{3}\right)\left(K_{Qs} e_{Qs} + \dot{Q}_{s-ref} - \omega_s P_s\right) \\ \frac{2}{3}(R_s L_r + R_r L_s) Qs + (R_r + \omega_r L_r)\left(v_{sd}\varphi_{sd} + v_{sq}\varphi_{sq}\right) \end{pmatrix} \end{cases} \tag{16}$$

Also, we find the virtual reference input:

$$\begin{cases} Q_{s\_ref} = Q_s \\ P_{s\_ref} = \frac{3}{2(R_s.L_r + R_r.L_s)}\begin{pmatrix} \left(\frac{2.\sigma.L_s.L_r}{3}\right).\left(-k_{P_s}.e_{P_s} + \omega_s.Q_{s\_ref}\right) \\ -\begin{pmatrix} (R_r + \omega_r.L_r).(v_{sd}.\psi_{sd} + v_{sq}.\psi_{sq}) \\ -M.(-v_{sd}.v_{rd} + v_{sq}.v_{rq}) + L_r.V_s^2 \end{pmatrix} \end{pmatrix} \end{cases} \tag{17}$$

B. Grid Side Converter Control

On the other hand, the control in the grid side ensures the stability of the amplitude voltage of the DC-link and maintains the unit power factor [10-15]. To do that, we express the errors [5-34], such as:

$$e_{V_{dc}} = V_{dc\_ref} - V_{dc} \tag{18}$$

$$\begin{cases} e_{P_g} = P_{g\_ref} - P_g \\ e_{Q_g} = Q_{g\_ref} - Q_g \end{cases} \tag{19}$$

$$V_1 = \frac{1}{2} e_{V_{dc}}^2 \tag{20}$$

$$V_2 = \frac{1}{2}\left(e_{V_{dc}}^2 + e_{P_g}^2 + e_{Q_g}^2\right) \tag{21}$$

As mentioned before, the derivative of Lyapunov functions (V_1 and V_2) must be negative. For this purpose, we introduce a positive constant in the derivative of (V_1 and V_2) [17]:

$$\dot{V}_1 = -K_{Vdc} e_{Vdc}^2 \leq 0 \tag{22}$$

$$\dot{V}_2 = -K_{Vdc} e_{Vdc} - K_{Ps} e_{Pq} - K_{Qs} e_{Qs} \leq 0 \tag{23}$$

After calculation, we obtain the vectors:

$$\begin{cases} v_{gd} = \frac{L_r}{\sqrt{\frac{3}{2}\hat{v}}}\left(K_{Ps} e_{Ps} + \dot{P}_{s-ref} + \frac{R_r}{L_r} P_s + \omega_s Q_s - \frac{1}{L_r}\left(v_{gd}^2 + v_{gq}^2\right)\right) \\ v_{gq} = \frac{L_r}{\sqrt{\frac{3}{2}\hat{v}}}\left(K_{Qs} e_{Qs} + \dot{Q}_{s-ref} + \frac{R_r}{L_r} Q_s + \omega_s P_s\right) \end{cases} \tag{24}$$

Also, we find virtual reference inputs:

$$\begin{cases} \boldsymbol{P}_{g\_ref} = \boldsymbol{P}_g \\ \boldsymbol{v}_{s\_ref} = \dfrac{\boldsymbol{P}_{g\_ref}}{\boldsymbol{C}.\boldsymbol{k}_{v_{dc}}.\boldsymbol{e}_{v_{dc}}} - \boldsymbol{P}_r \end{cases} \tag{25}$$

5) DFIG Parameters Estimation

To approach reality, we will use observers to estimate the machine parameters and the load torque; this will help us to develop the real model of the machine. By developing such a model, we will improve the robustness of the control to parameter variations and measurement noise. Next, to design the adaptive nonlinear Backstepping control, we will replace the vectors of the real parameters of the DFIG with their estimates. The expressions of the powers will be [15]:

$$\begin{cases} \dot{e}_{Ps} = \dot{P}_{s-ref} + \hat{a}_2 P_s + \begin{pmatrix} \hat{a}_3\left(v_{sd}\varphi_{sd} + v_{sq}\varphi_{sq}\right) \\ +\hat{a}_4\left(-v_{sd}v_{sq} + v_{rd}v_{rq}\right) + \hat{a}_5 V_s^2 - Q_s\omega_s \end{pmatrix} \\ \dot{e}_{Qs} = \dot{Q}_{s-ref}\left(\hat{a}_2 Q_s + \begin{matrix} \hat{a}_3\left(v_{sd}\varphi_{sd} + v_{sq}\varphi_{sq}\right) \\ +\hat{a}_4\left(-v_{rd}+v_{rq}\right)v_{sd} - Q_s\omega_s \end{matrix}\right) \end{cases} \tag{26}$$

$$\hat{a}_2 = \left(\frac{\hat{R}_s.\hat{L}_r + \hat{R}_r.\hat{L}_s}{\hat{\sigma}.\hat{L}_s.\hat{L}_r}\right) \quad \hat{a}_3 = \left(\frac{3.\left(\hat{R}_r + \omega_r.\hat{L}_r\right)}{2.\hat{\sigma}.\hat{L}_s.\hat{L}_r}\right) \quad \hat{a}_4 = \left(\frac{3.M}{2.\hat{\sigma}.\hat{L}_s.\hat{L}_r}\right) \quad \hat{a}_5 = \left(\frac{3}{2.\hat{\sigma}.\hat{L}_s}\right) \tag{27}$$

In this work, we will focus on the variations of the parameters *Rs*, *Rr*, *Ls*, *Lr*, and *σ*. Though, it will be easy to estimate the *M*. Similarly if the *Ls* and the *Lr* vary the *M* also varies. After, a new Lyapunov function V_2 will be defined using gain adaptation:

$$V_2 = \frac{1}{2}\left(e_\Omega^2 + e_{P_s}^2 + e_{Q_s}^2 + \frac{\tilde{C}_m^2}{\gamma_m} + \frac{\tilde{a}_1^2}{\gamma_1} + \frac{\tilde{a}_2^2}{\gamma_2} + \frac{\tilde{a}_3^2}{\gamma_3} + \frac{\tilde{a}_4^2}{\gamma_4} + \frac{\tilde{a}_5^2}{\gamma_5}\right) \tag{28}$$

We will also maintain the derivative of the equation (28) equal to zero, to guarantee the system stability. From the calculation procedure, we recommend the following control laws (V_{rd} and V_{rq}):

$$\begin{cases} v_{rd} = \frac{1}{\hat{a}_4 v_{sd}}\begin{pmatrix} K_{Ps} e_{Ps} + \dot{P}_{s-ref} + \hat{a}_2 P_s - \omega_s Q_s \\ +\hat{a}_3\left(v_{sd}\varphi_{sd} + v_{sq}\varphi_{sq}\right) + \hat{a}_5 V_s^2 \end{pmatrix} + \frac{v_{sq}}{v_{sd}} v_{rq} \\ v_{rq} = \frac{1}{\hat{a}_4 v_{sd}}\begin{pmatrix} -K_{Qs} e_{Qs} + \dot{Q}_{s-ref} - \hat{a}_2 Q_s - \omega_s P_s \\ -\hat{a}_3\left(v_{sd}\varphi_{sd} + v_{sq}\varphi_{sq}\right) \end{pmatrix} + v_{rd} \end{cases} \tag{29}$$

From equation (29), we find the adaptation expressions of the DFIG-parameters as follows:

6) The stator and rotor resistances:

$$\begin{cases} \tilde{R}_r = \int \dot{\tilde{R}}_r = \int \frac{2\dot{\tilde{\sigma}}\tilde{L}_s\tilde{L}_r\tilde{a}_3}{3} - \omega_r\dot{\tilde{L}}_r \\ = \frac{2}{3}\int \dot{\tilde{\sigma}}\tilde{L}_s\tilde{L}_r - \gamma_3\left(v_{sd}\varphi_{sd} + v_{sq}\varphi_{sq}\right)\left(e_{Ps} + e_{Qs}\right) - \omega_r\dot{\tilde{L}}_r \\ \tilde{R}_s = \int \dot{\tilde{R}}_s = \int \frac{\dot{\tilde{\sigma}}\tilde{L}_s\tilde{L}_r\tilde{a}_2 - \tilde{R}_r\tilde{L}_s}{\tilde{L}_r} \\ = \int \gamma_2\dot{\tilde{\sigma}}\tilde{L}_s\left(-e_{Ps}P_s - e_{Qs}Q_s\right) - \frac{\tilde{L}_s}{\tilde{L}_r}\dot{\tilde{R}}_r \end{cases} \tag{30}$$

7) The stator and rotor inductances:

$$\begin{cases} \tilde{L}_r = \int \dot{\widetilde{L_r}} = \int \sqrt{\left(\frac{1}{\dot{\widetilde{a_1}}}\right)} = \int \sqrt{\left(-\frac{1}{\gamma_1 e_\Omega \left(\frac{2pM^2}{3Jv_S}\right)(\varphi_{sq}Q_S+\varphi_{sd}P_S)-\frac{pM}{J}\varphi_{sq}\varphi_r}\right)} \\ \tilde{L}_s = \int \dot{\widetilde{L_s}} = \int \frac{3}{2\dot{\tilde{\sigma}}\dot{\widetilde{a_5}}} = \frac{3}{2\gamma_5 V_{\tilde{S}}^2}\int \frac{1}{\dot{\tilde{\sigma}} e_{Ps}} \end{cases} \quad (31)$$

5. Rooted Tree Optimisation Algorithm

A. Principle

The development of bases and services for trees under the ground is very connected to its root framework. From this perspective, the practices of the roots under the ground have become a cutting-edge innovation [11]. This implies that the primary of the tree gives various roots to begin the pursuit. It is the hub principal gathering of arbitrary arrangements. The upcoming generation is acquired from the assessment of the principal assortment as per the root nearest to the corn and the level of fineness, and the roots which are a long way from the corn are eliminated.

The technique of this calculation is to follow the comportment of the underlying foundations of trees looking for groundwater as per the level of underground control.

Based on this principle, it makes it possible to infer another calculation. To apply this calculation, the factors must be clarified.

Wetness Degree (Dw): decides the level of actual wellness between the populace. Also, the factors (Rr, Rc, Rn) are the rates that affect the admittance to the arrangement.

The roots of the trees will search for the best arrangement or the closest spot for the beginning of the new populace. The random root (Rr) is the nearest one to the water. The individuals from the new populace - the new generation - are beginning arrangements proposed [15]. The new populace is determined dependent on this:

$$\mathrm{Y^{new}(k, i_{t+1}) = Y_r(i_t) + b_3.D_w(k).randn.\frac{m}{t}} \quad (32)$$

Depending on the choice of the nearest roots (Rn) close to the water which gathers around the humid place from which a new generation is created, but the roots away from moisture are removed. Considering the number of candidates, the following expression is assumed to ascertain the new generation.

$$\mathrm{Y^{new}(k, i_{t+1}) = Y^{mei}(i_t) + b_1.D_w(k).randn.\frac{m}{N.i_t}} \quad (33)$$

The new generation is made by roots that have assembled around the closest place to the water whose continuity root (Rc). A new generation of the population is determined by the next equation.

$$\mathrm{Y^{new}(k, i_{t+1}) = Y(k, i_t) + b_2.D_w(k).randn.\left(Y^{mei}(i_t) - Y(k, i_t)\right)} \quad (34)$$

B. RTO applied to the Backstepping Control to DFIG

For this, the determination of the optimal gains of the Backstepping algorithm with integral (BSI) in the DFIG command must first follow certain steps.

- **Step 1 :**

To determine the first generation from the input values for the following variables: The variables (Rr, Rc, Rn). Knowing that ($Rr + Rc + Rn$ = 100% = 1), then the number of candidates N is definite.

- **Step 2:**

From the initial step (Fig.2), we can figure the degree of wetness for the whole primary generation. Then, we assign the control degree (Dw) as in (35). At that point, we take the best wetness degree of the generation's members [15].

$$D_w(k) = \begin{cases} \frac{f_k}{max f_k} \; for\ maximal\ objective \\ 1 - \frac{f_k}{max f_k} \; for\ minimale\ objective \end{cases} \quad (35)$$

- **Step 3:**

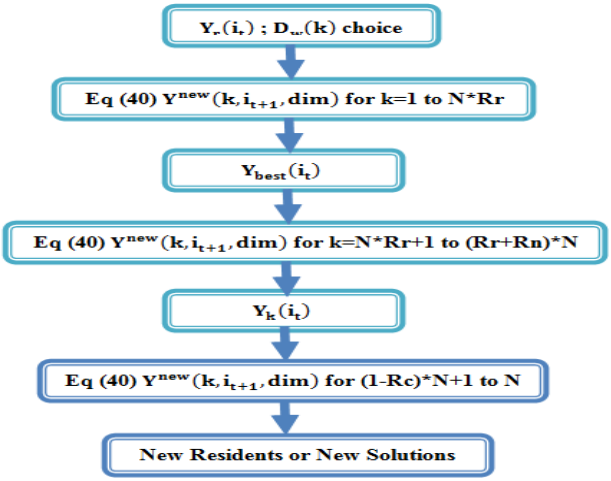

Fig.2. Step 3 Algorithm

- **Step 4:**

If the stop criteria are not matched, we go back to step 2.

- **Step 5:**

If the maximum of iterations is reached, we go to step 6.

- **Step 6:**

The best solution is the individual that gives us the optimal values for DFIG control using BSI regulator (Fig.3) [16].

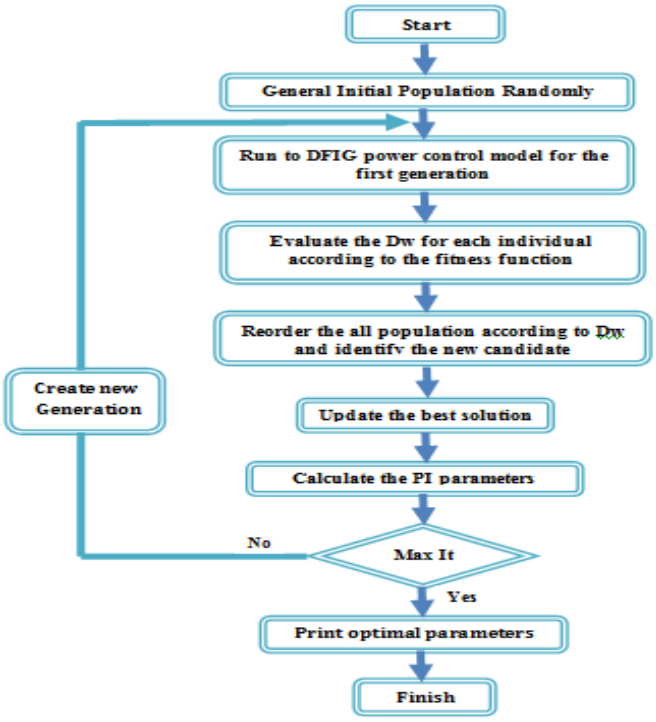

Fig.3. RTO Optimization Algorithm

Table 1: RTO Parameter

Parameters	Values
RTO Size	20
Maximum number of iterations	20
$B_1=b_2=b_3$	2
$R_n=R_r$	0.2
Rc	0.4
Dm	2

6. Results and Discussion

Figure 4 show the scheme proposed to apply the adaptive non-linear Backstepping control to a DFIG-WECS. The wind system is subjected to a series of simulation tests under the MATLAB / SIMULINK environment to assess the performance, robustness, and stability of the active and reactive power control of the DFIG.

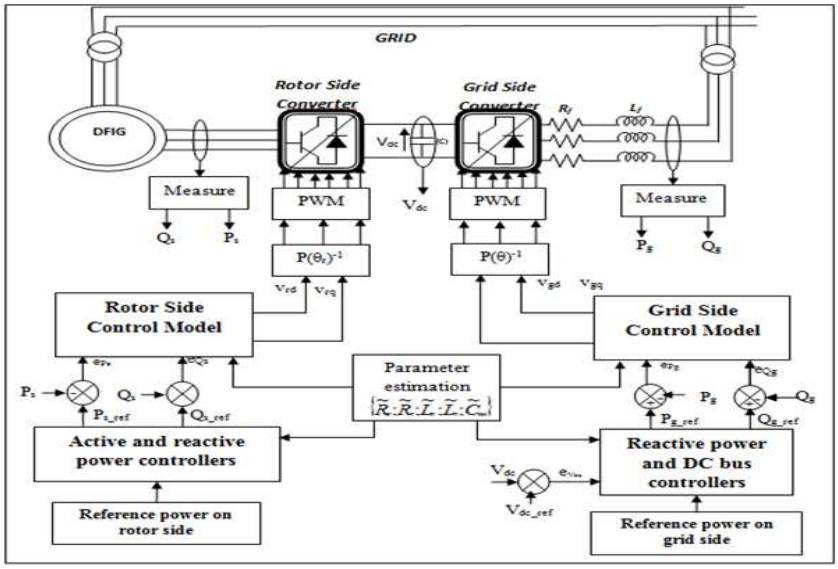

Fig. 4. Backstepping control applied to DFIG

A. Performance Test

In this part, we focus on analyzing the behavior of DFIG toward the random wind profile. The reactive power is set to zero (Qs_ref = 0 Var) to guarantee a unit power factor and to enhance the quality of the energy injected into the electrical grid. The simulations were carried out using a real wind profile. The results of the adaptive Backstepping control applied to DFIG are gathered in the next figures.

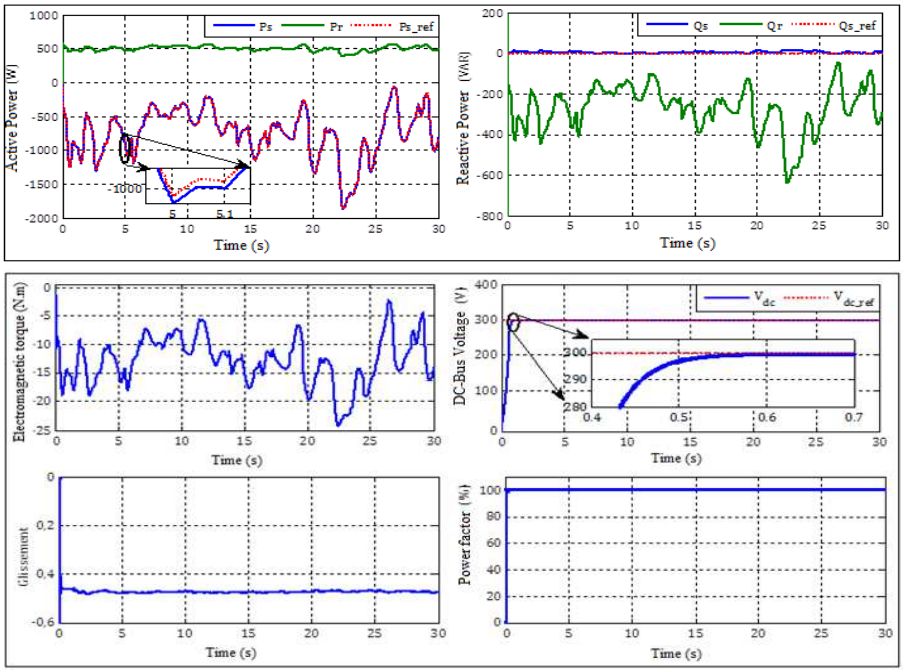

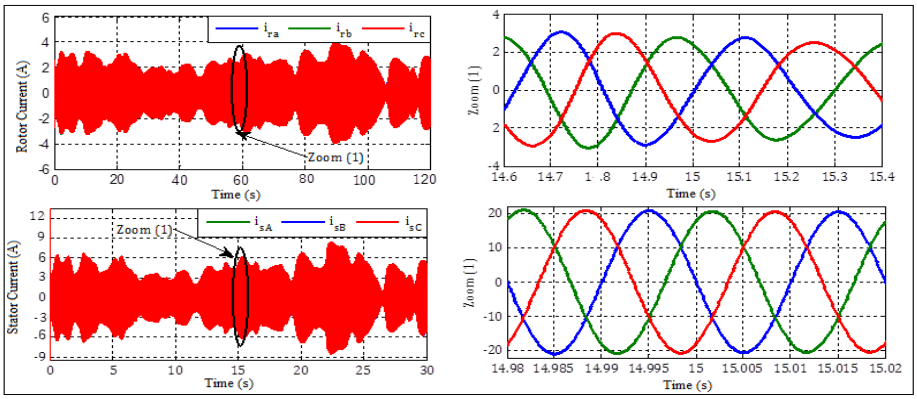

Fig. 5. Variable Wind speed system response

Figure 5 shows that the active power pursuits its reference value generated by the MPPT strategy with a dynamic error of ε= 1.05%. The reactive power is always maintaining its value which is zero, thus confirming that the power factor is equal to one under steady-state. The electromagnetic torque of the generator fluctuates following the speed turbine which is a mirror image of the wind speed. The power oscillations are insignificant comparing to those of the electromagnetic torque. Also, the DC link shows a fast and precise dynamic, it reaches its reference value at tV_{dc} = 0.55 s with no overshoot and with a small static error. The stator currents vary along with the wind variation. Despite the variations of the wind, these currents are sinusoidal with a frequency of 50Hz. The rotor currents have also the same shape and their frequency is proportional to the mechanical speed. These currents have fewer undulations in comparison with other techniques.
Figure (6) shows the spectrum of the stator and rotor currents.

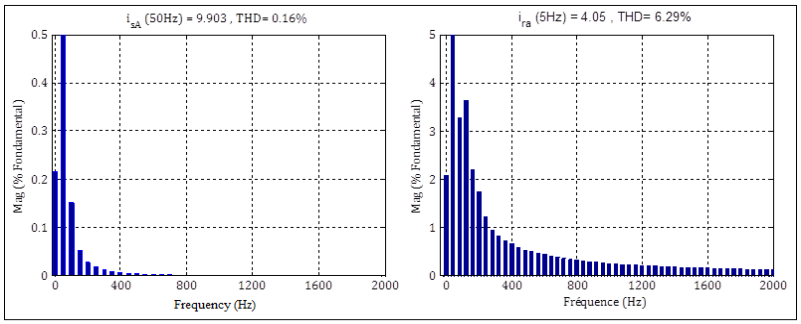

Fig.6. analyzed the harmonics of the spectra of currents at variable wind speed
The THD is clearly (6.29%) for the rotor current instead of (0.16%) for the stator current.

B. Robustness Test

To check the performance and stability of the adaptive Backstepping control on the regulation of the active and reactive powers, some modifications are made at the level of the internal DFIG parameters of the model used.
Various tests are made by increasing or decreasing the machine parameters: the stator and the rotor resistances and inductances. The following figures show the dynamic behaviour of the system:

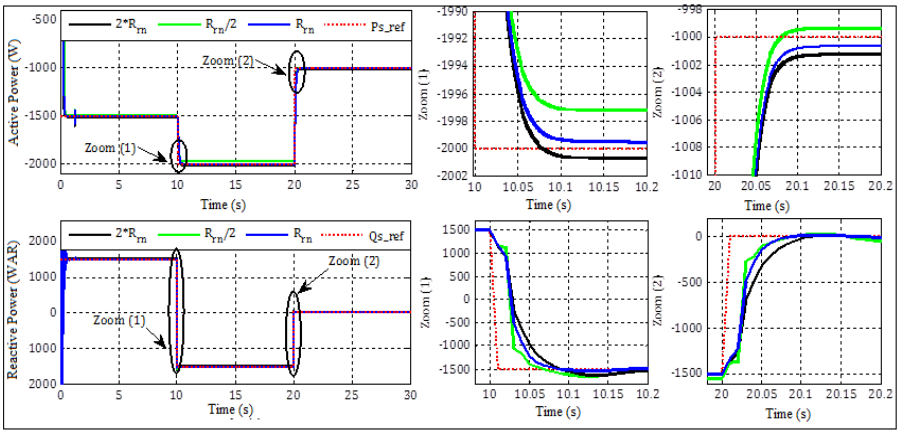

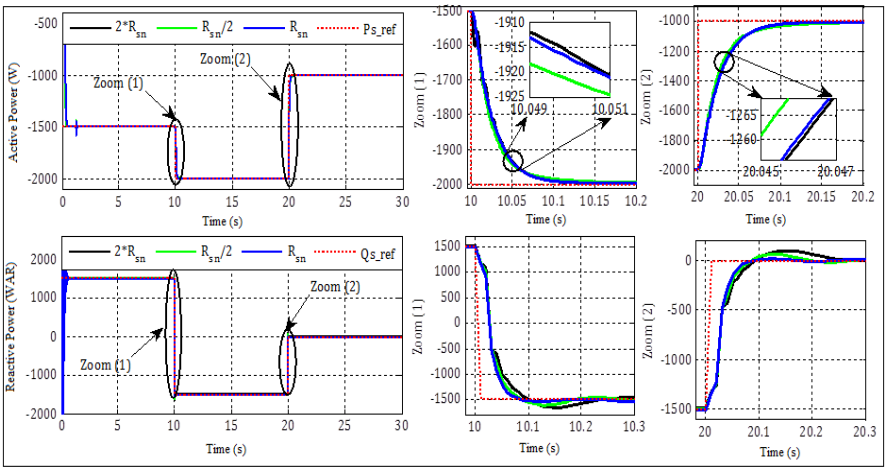

Fig.7. Robustness test during resistance variation

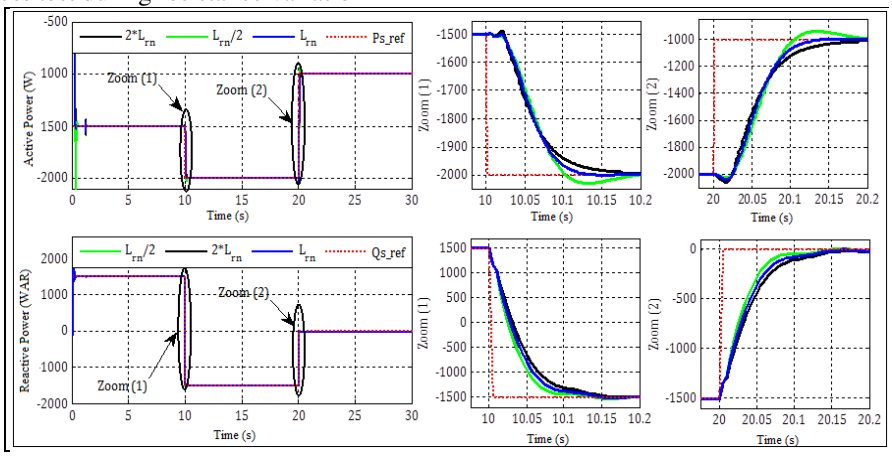

Fig.8. Robustness test during inductance variation

Based on these results, it should be noted that the active and reactive powers tracked the references imposed. However, we detect a minor rise in the response time due to the changes applied to the stator and rotor resistances (figure 7). The static error is nearly zero with little ripples. On the other hand, the variations of the rotor and stator inductances (figure 8) generate the same response time and low sensitivity during the pursuit of the setpoint. The decoupling between active and reactive powers is always ensured. In conclusion, the adaptive Backstepping command is robust regardless of the parameter variations stated before.

7. Experimental validation

Before validating the performance of the non-linear Backstepping control on an experimental bench, the control algorithm will be implemented in a DS1104 R&D card developed by dSPACE. This card is linked to a computer via an interface that helps us to transfer data between the software and the hardware parts. The hardware part of the dSPACE card generates PWM signals in TTL 0/5V. The software part is the environment Matlab / Simulink which converts the model developed using blocks in the 'Toolbox Real-Time Interface (RTI) library that configures the inputs/outputs of the system proposed to a real-time algorithm in C language (Figure 9).

Then, the program source built will be load into the “ControlDesk” and the data acquisition to run the system will be sent from the sensors and presented graphically.

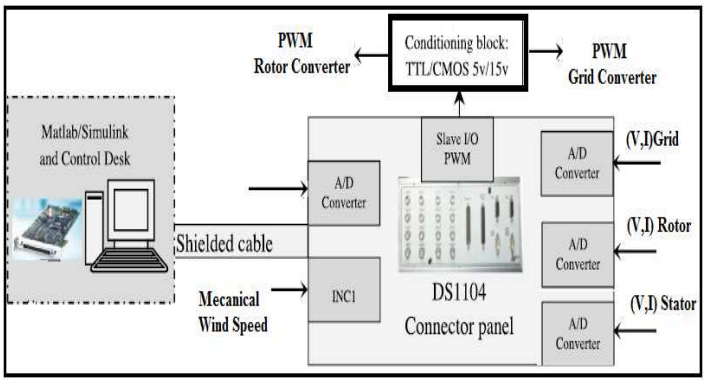

Fig. 9. dSPACE connection diagram with the wind system

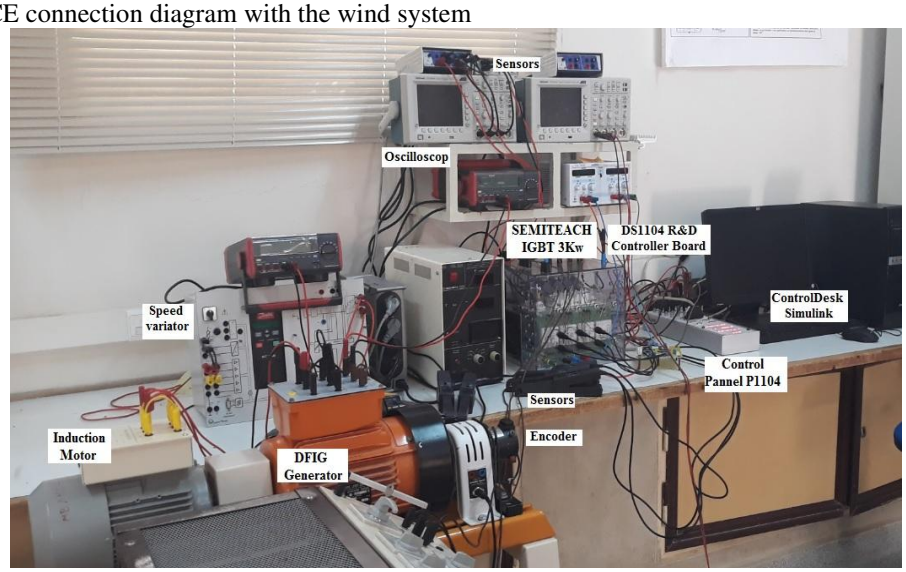

Fig. 10. Experimental Benchmark of Wind Turbine System

Figure 10 presents the test bench for the validation of the proposed control strategy. It is composed of:

- A doubly fed induction generator DFIG **1.5kW** (the parameters are detailed in the Table 2)
- An induction motor to drive the DFIG, it plays the role of the turbine and which is driven by a variable speed coming from a variable speed drive (to generate a variable wind speed).
- A Semikron Inverter (SEMITEACH IGBT **3kW**) is connected to the dSPACE card via an isolation and adaptation card.

We chose a real wind profile, which is generated by a speed controller connected to the DFIG drive motor. Figure 11 shows the results acquired of the adaptive Backstepping control:

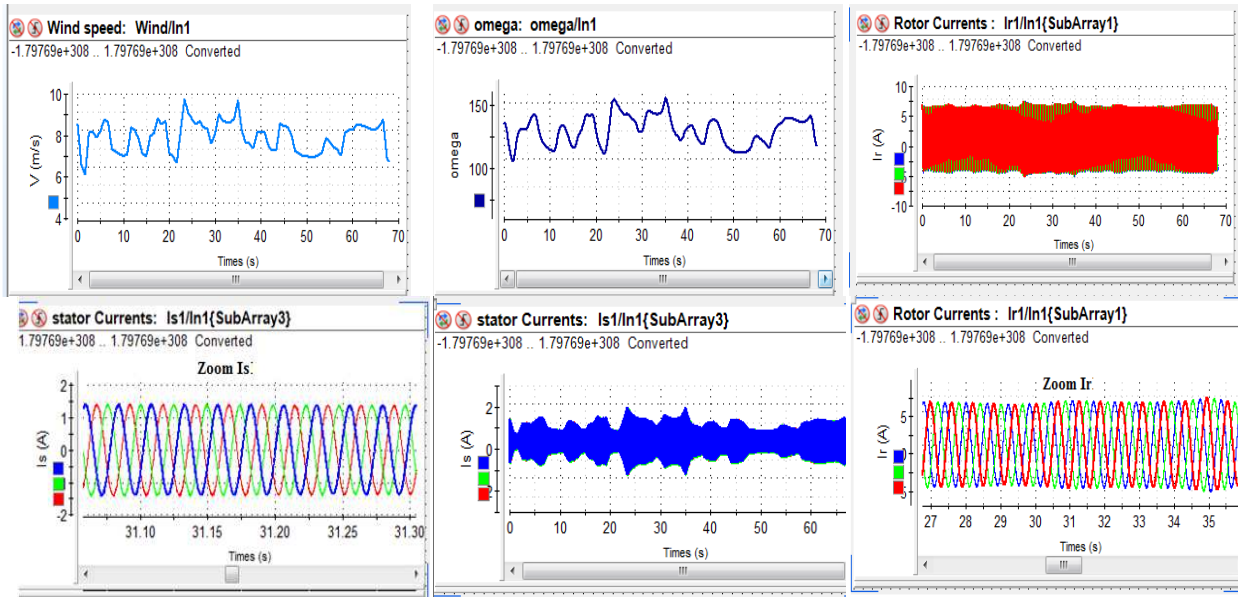

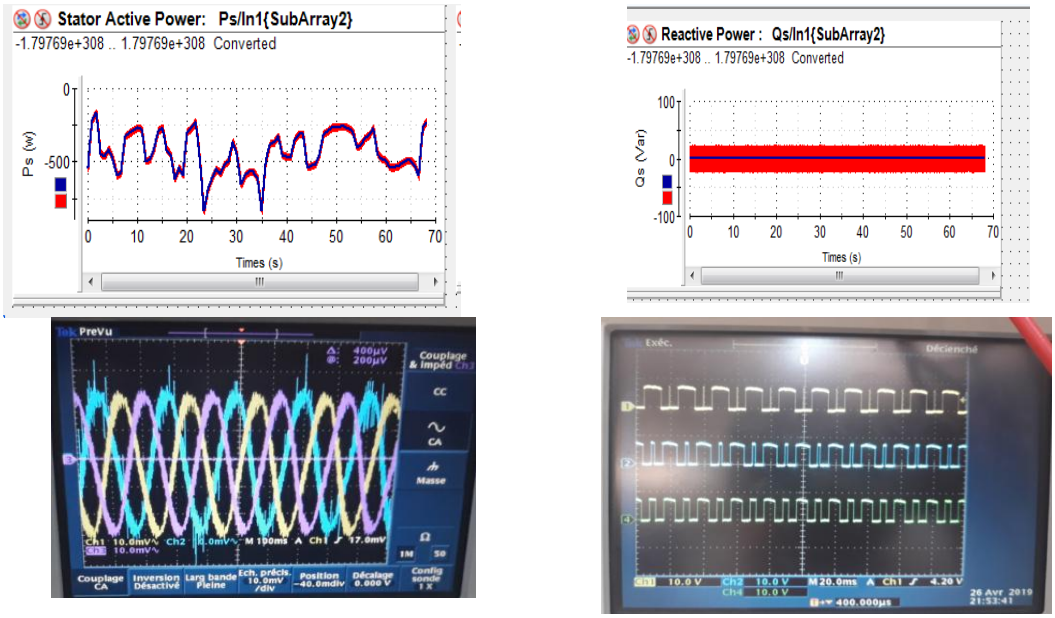

Fig. 11. Experimental results of the Backstepping control applied to a WECS

The results obtained (Figure 11) clearly show good monitoring of active and reactive powers with their references. Also, the mechanical speed follows, with small ripples, the wind speed. These ripples are due to the fluctuation of the wind speed. The reactive power is reasonably low compared to the total power generated. Its value is around 20 VAR that provides a power factor close to one.

Moreover, the stator and rotor currents show a perfect waveform sinusoidal with a frequency of 50Hz in the stator side and a rapid tracking response. We can observe that the experimentation results correspond to those obtained in the simulation part either in terms of response time or in the quality of the waves of electrical currents. The adaptive nonlinear Backstepping control gives remarkable results: reduced response time and good tracking of references (Table 1).

To sum up, we can say that the results of the validation of the Backstepping control show a good correlation between the experiment and simulation.

Table 1 : Performance comparison.

Publication	Technic methods	Efficiency	Error	Overshot	Cos φ	« Robustness »
N. Bounar et al-2014	Adaptive Fuzzy Vector Controller	93.5	0,15 %	0 %	0.997	Moderate-high
	Adaptive Fuzzy Controller	93.99	0,14 %	0 %	0.974	Moderate-high
Z. Abderrahim et al-2016	DTC-classical	92.13	0,32 %	5 %	0.983	Moderate-high
	DTC-GA-based PI	92.07	0,12 %	1 %	0.978	Moderate-high
S, Abderazak et al-2016	Sliding mode	94.82	0,2 %	0 %	0.972	Low
Proposal technique	Backstepping adaptative	98.99	0,12 %	0 %	0.995	High

Table 2 : DFIG and WT parameters.

DFIG			WT		
Parameters	**Symbol**	**Values**	**Parameters**	**Symbol**	**Values**
Power Generator	Ps	1.5 KW	Radius	R	20 m
Stator Resistance	Rs	4.85 Ω	Density of air	ρ	1.22 kg/m3
Rotor Resistance	Rr	3.805 Ω	Optimal Tip-speed ratio	λopt	8
Stator Inductance	Ls	274 mH	Maximum of power coefficient	Cp	0.45
Rotor Inductance	Lr	258 mH			

8. Conclusion

This paper discussed a non-linear control applied to a WECS-DFIG. The Backstepping Adaptive control based on the Lyapunov stability technique is developed to make WECS works in better conditions. To demonstrate its efficiency, we simulate the whole system using Matlab / Simulink tool that provides satisfying results in terms of pursuits and parameter variations. The second part was dedicated to testing the same model on an experimental test bench with an implementation in the DS1104. The experimental results were able to achieve the majority of the objectives discussed in the simulation part. The significant findings of this work are:

- ✓ Adaptive Backstepping control offers good performances under a real wind profile.
- ✓ The robustness despite the variations of the wind profile and the machine parameters is well-ensured thanks to this control algorithm.
- ✓ The simulation results show that the Backstepping control strategy, applied to a wind energy conversion system, realized an excellent performance.
- ✓ The experimental results show a perfect correlation with the simulation results.

In further work, we will analyze the dynamic performance of a WECS-DFIG linked to the electrical grid and try to resolve the problems of voltage drops and flickers.

Nomenclature

f_r, f_s: Frequency at rotor and stator
Ω_t: turbine speed
R_s, R_r: Resistances of the stator/rotor
R_f, L_f: Resistances and inductance of a phase of the filter
L_r, L_s: Inductances of the stator / rotor.
P_s, P_r, P_g: Active power at stator, rotor, and grid
Q_s, Q_r, Q_g: Reactive power to stator, rotor, and network
P_{mec}, P_{res}, P_{elec}: Mechanical, network and electrical power
P_{ins}, P_{ext}: recoverable wind and theoretical power
T_{em} , C_{em} : Electromagnetic torque
C_r : Load torque available at a motor shaft
$V_{r(a,b,c)}$, $V_{s(A,B,C)}$: Rotor and stator voltages
$i_{r(a,b,c)}$, $i_{s(A,B,C)}$: Rotor and stator currents
$\psi_{r(a,b,c)}$, $\psi_{s(A,B,C)}$: Rotor and stator Flux
$(v_{sd}$, $v_{sq})$, $(i_{sd}$, $i_{sq})$: d/q stator voltages and currents
$(v_{rd}$, $v_{rq})$, $(i_{rd}$, $i_{rq})$: d/q rotor voltages and currents
$(v_{gd}$, $v_{gq})$, $(i_{gd}$, $i_{gq})$: Grid voltages and currents
(v_{td}, v_{tq}), $(i_{td}$, $i_{tq})$: Voltages and currents at the RL filter

9. Acknowledgement:

Taif University Researchers Supporting Project number (TURSP-2020/10), Taif University, Taif, Saudi Arabia.

10. References

[1] Bossoufi, B., Karim, M., Lagrioui., 2015. Observer Backstepping control of DFIG-generators for wind turbines variable-speed: FPGA-based implementation. Renewable Energy 81, 903–917.

[2] Abderrahim Zemmit, Sabir Messalti, Abdelghani Harrag,'' A new improved DTC of doubly fed induction machine using GA-based PI controller'', Ain Shams Engineering Journal, PP, 1-9, October 2016,

[3] Y. EL Mourabit , A.Derouich, A.EL Ghzizal, J. Bouchnaif, N.EL Ouanjli, B.Bossoufi, "Implementation and validation of backstepping control for PMSG wind turbine using dSPACE controller board" Energy Report Journal (Elsiver), pp 807-821, Vol. 5. September 2019.

[4] N. EL Ouanjli, A.Derouich, A.EL Ghzizal, J. Bouchnaif, M.Taoussi, B.Bossoufi "Real-time Implementation in dSPACE of DTC-Backstepping for Doubly Fed Induction Motor" European Physical Journal Plus, Vol 135, No1, pp 2-9, October 2019.

[5] D. Seyoum, C. Grantham, «Terminal Voltage Control of a Wind Turbine Driven Isolated Induction Generator using Stator Oriented Field Control». IEEE Transactions on Industry Applications, pp. 846-852, September 2003.

[6] Bossoufi, B., Karim, M., Lagrioui, A., Taoussi, M., El Hafyani, M.L., 2014b. Backstepping control of DFIG generators for wide-range variable-speed wind turbines. Int. J. Autom. Control 8 (2), 122–140.

[7] Z. Zhang, Y. Zhao, W. Qiao and L. Qu, "A Space-Vector-Modulated Sensorless Direct-Torque Control for Direct-Drive PMSG Wind Turbines," in IEEE Trans on Industry Applications, vol. 50, no. 4, pp. 2331-2341, July-Aug. 2014.
[8] B. Beltran, M. E. H. Benbouzid and T. Ahmed-Ali, "Second-Order Sliding Mode Control of a Doubly Fed Induction Generator Driven Wind Turbine," in IEEE Trans on Energy Conversion, vol. 27, no. 2, pp. 261-269, June 2012.
[9] Bo Yang, Tao Yu, Hongchun Shu,Jun Dong,Lin Jiang, 2018. Robust Sliding-mode Control of Wind Energy Conversion Systems for Optimal Power Extraction via Nonlinear Perturbation Observers. Applied Energy (Elsivier) 210, 711-723.
[10] B. Beltran, T. Ahmed-Ali and M. E. H. Benbouzid, "High-Order Sliding-Mode Control of Variable-Speed Wind Turbines," in IEEE Transactions on Industrial Electronics, vol. 56, no. 9, pp. 3314-3321, Sept. 2009.
[11] Benamor, A., Benchouia, MT, Srairi, K. and Benbouzid, MEH, 2019. A new rooted tree optimization algorithm for indirect power control a wind turbine based on a powered double induction generator. ISA Transactions, 88, pp.296-306
[12] Mahela, O.P., Shaik, A.G., 2016. Comprehensive overview of grid interfaced wind energy generation systems. Renew. Sustain. Energy Rev. 57, 260–281.
[13] Matraji, I., Al-Durra, A., Errouissi, R., 2018. Design and experimental validation of enhanced adaptive second-order SMC for PMSG-based wind energy conversion system. Int. J. Electr. Power Energy Syst. 103, 21–30.
[14] Dogan, E., Seker, F., 2016. The influence of real output, renewable and non-renewable energy, trade and financial development on carbon emissions in the top renewable energy countries. Renew. Sustain. Energy Rev. 60, 1074–1085.
[15] D. Seyoum, C. Grantham, «Terminal Voltage Control of a Wind Turbine Driven Isolated Induction Generator using Stator Oriented Field Control». IEEE Transactions on Industry Applications, pp. 846-852, September 2003.
[16] Domínguez, J.A., Dufo-López, R., Yusta-Loyo, J.M., Artal-Sevil, J.S., Bernal- Agustín, J.L., 2019. Design of an electric vehicle fast-charging station with integration of renewable energy and storage systems. Int. J. Electr. Power Energy System. 105, 46–58.
[17] Dragomir, G., Şerban, A., Năstase, G., Brezeanu, A.I., 2016. Wind energy in Romania: A review from 2009 to 2016. Renew. Sustain. Energy Rev. 64, 129–143.
[18] Zhang, H.B., Fletcher, J., Greeves, N., Finney, S.J., Williams, B.W., 2011. Onepower point operation for variable speed wind/tidal stream turbines with synchronous generators. IET Renew. Power Gener. 5 (1), 99–108.

Figures

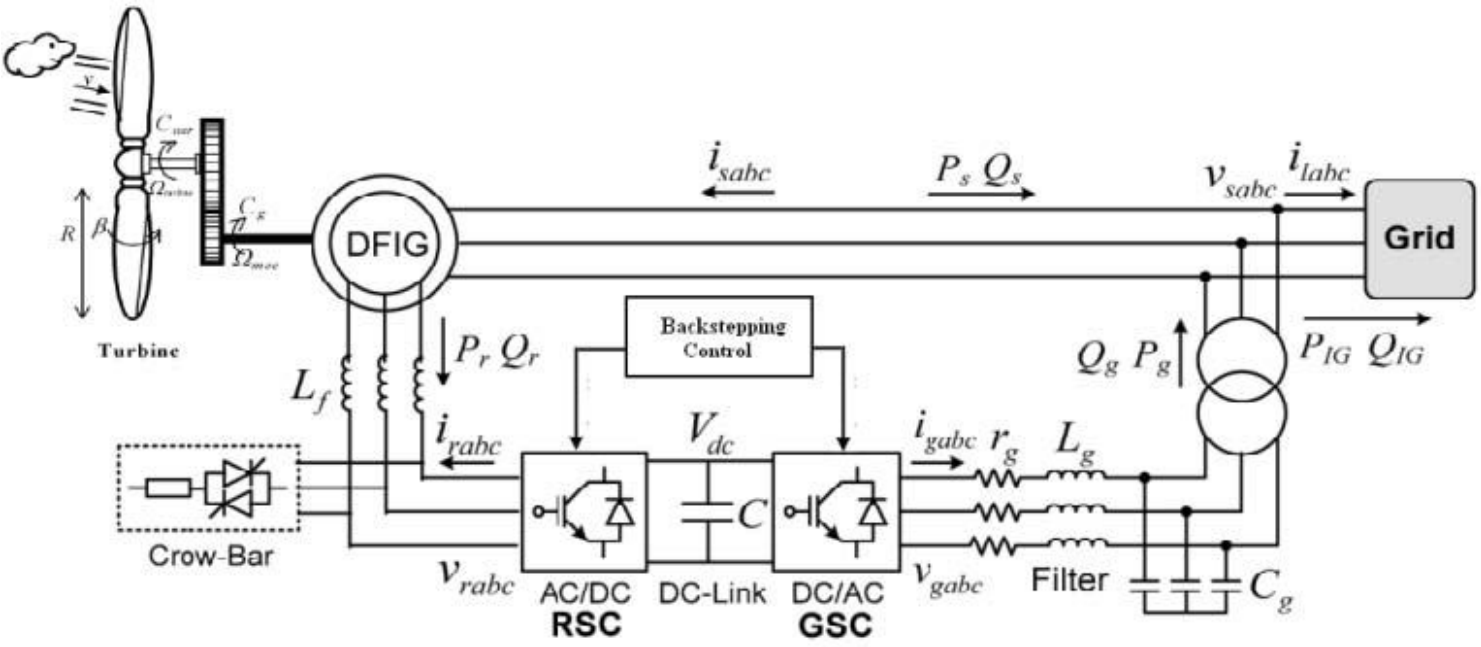

Figure 1

Wind power system structure

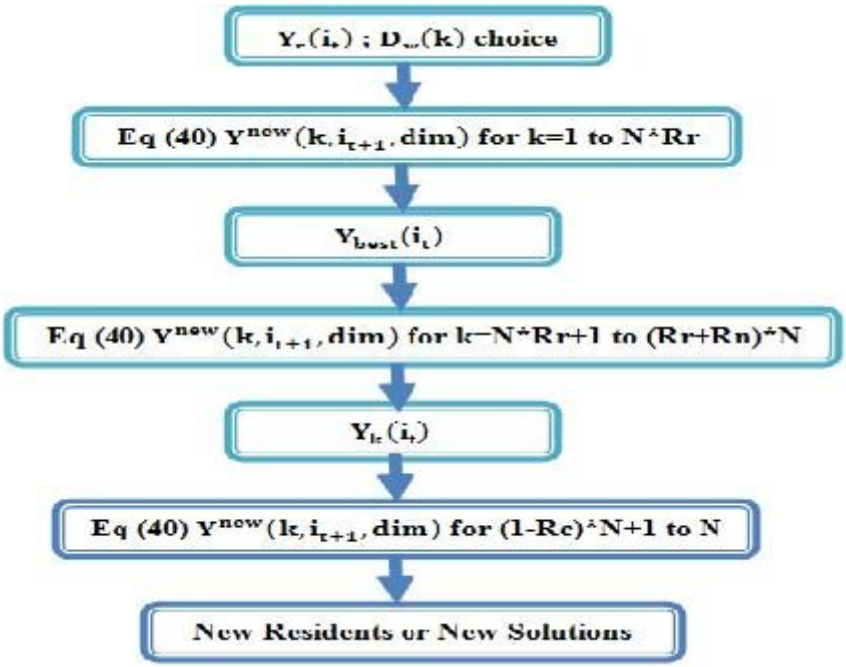

Figure 2

Step 3 Algorithm

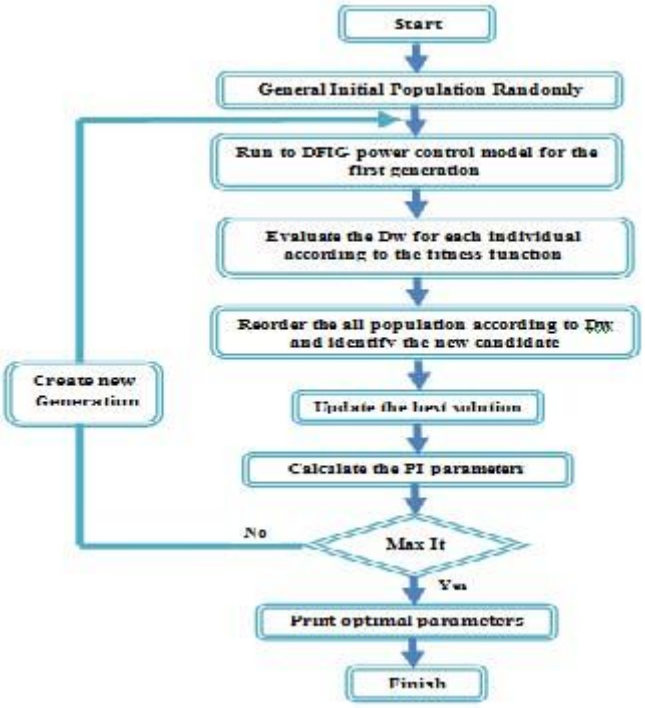

Figure 3

RTO Optimization Algorithm

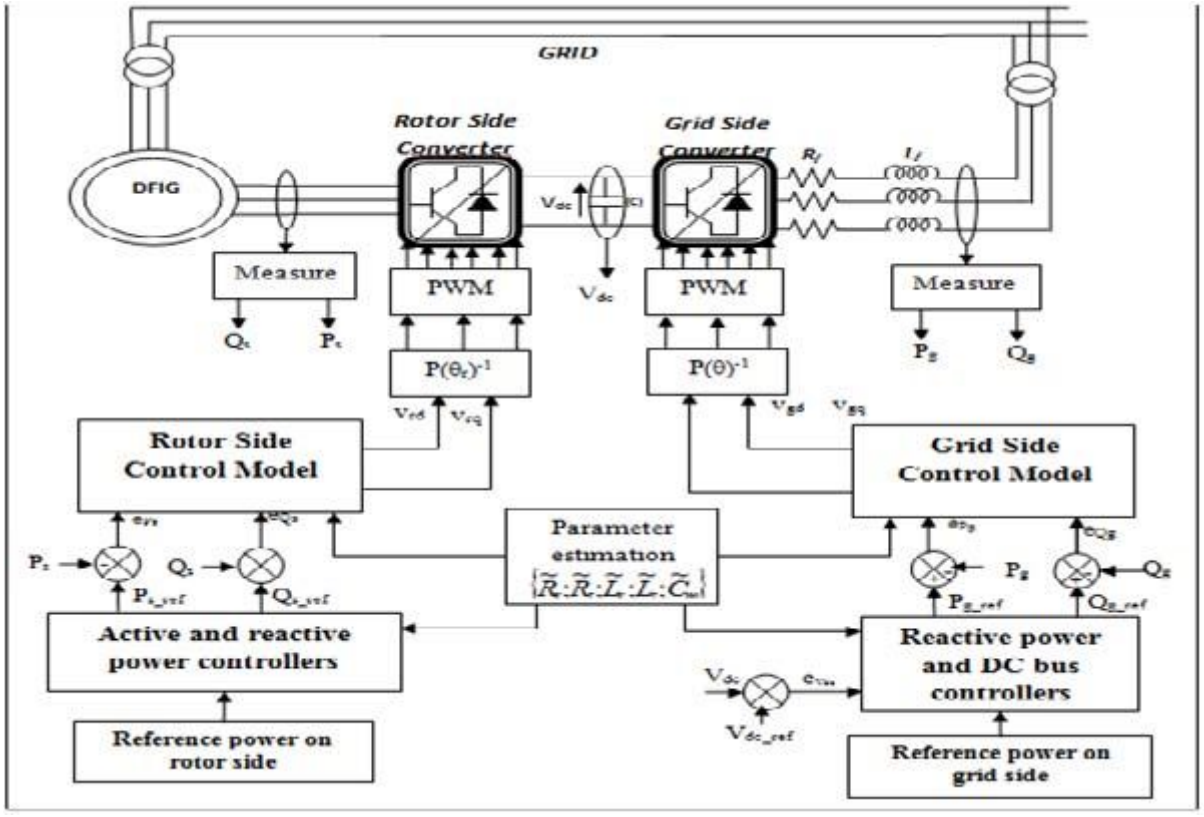

Figure 4

Backstepping control applied to DFIG

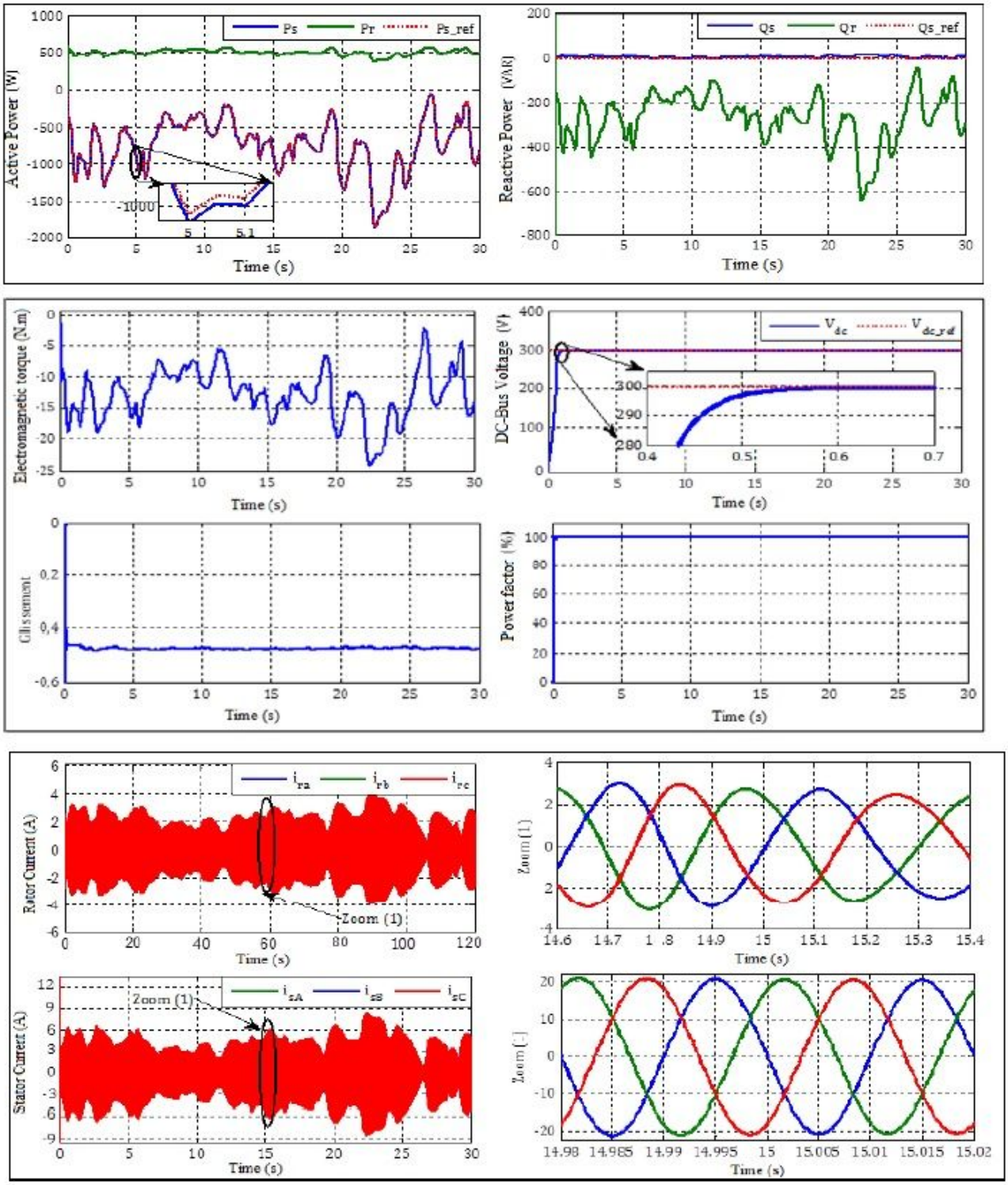

Figure 5

Variable Wind speed system response

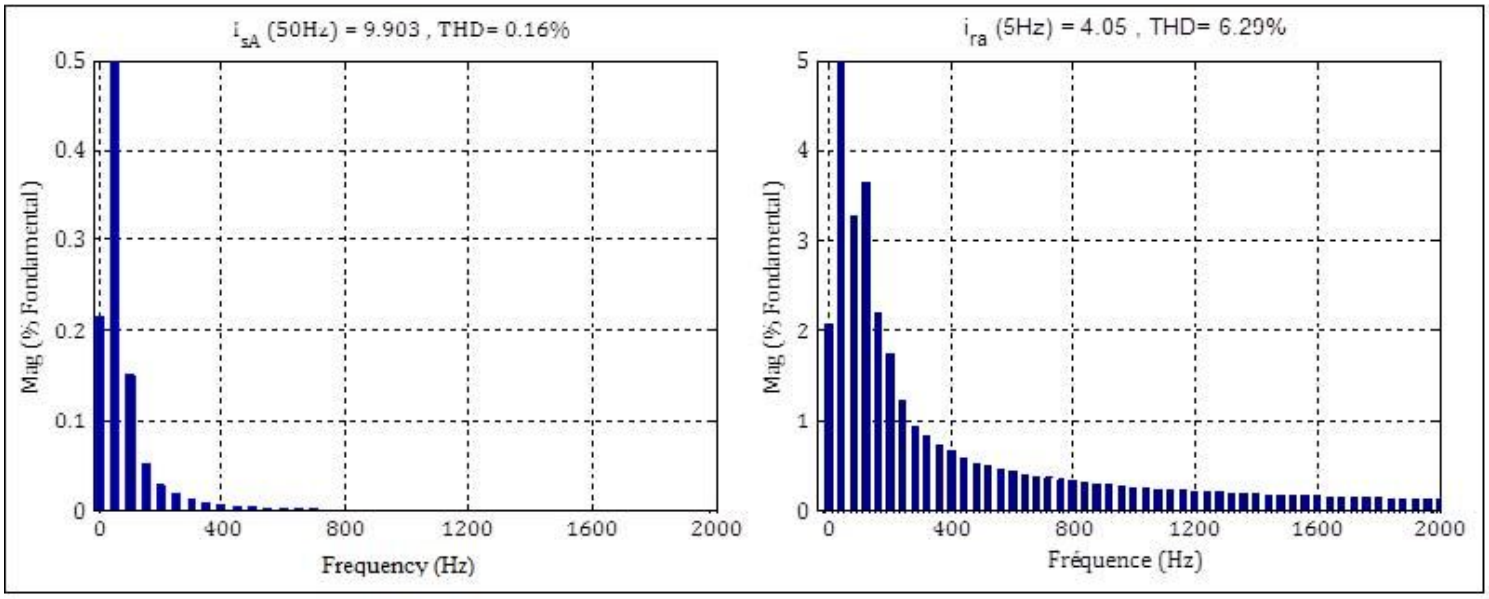

Figure 6

analyzed the harmonics of the spectra of currents at variable wind speed

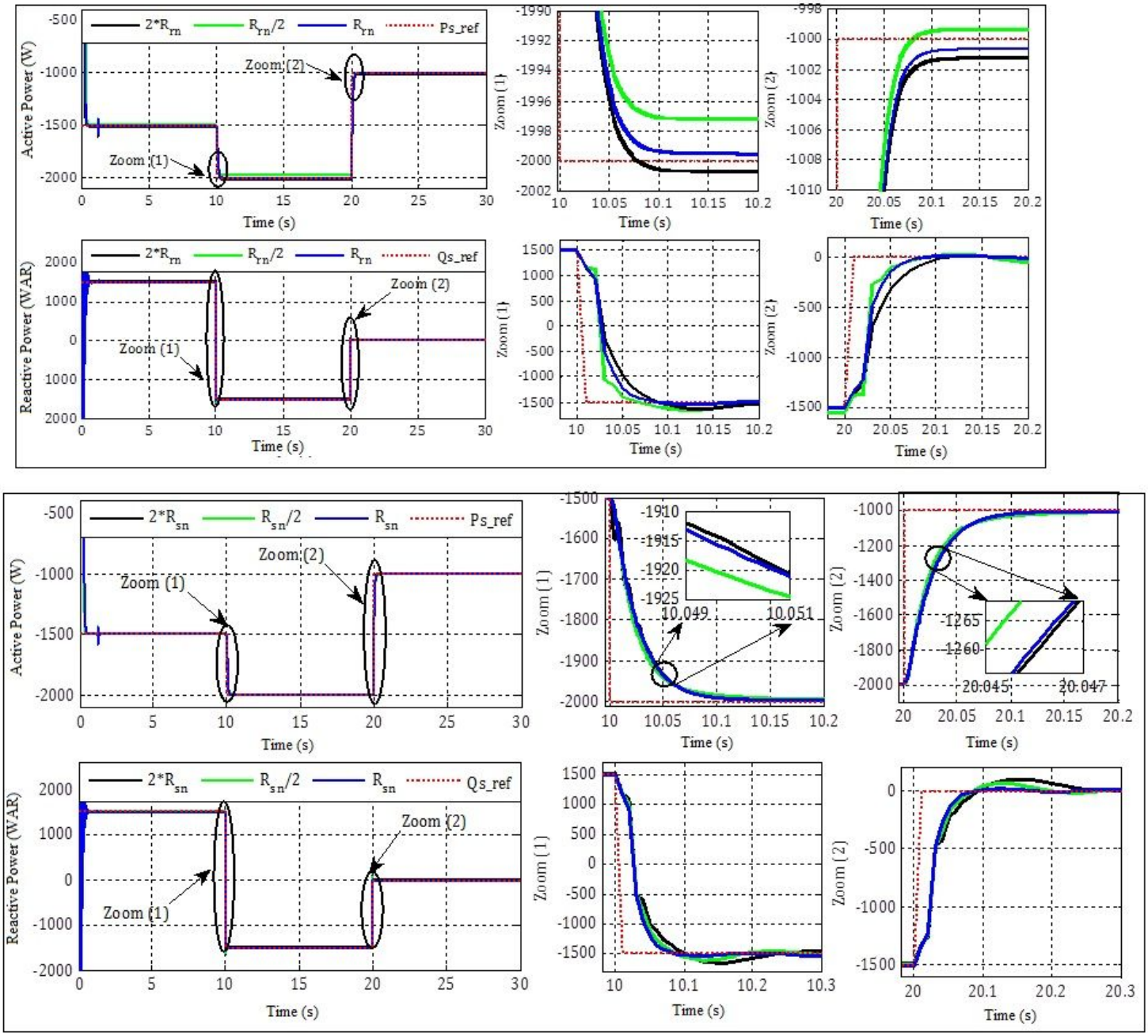

Figure 7

Robustness test during resistance variation

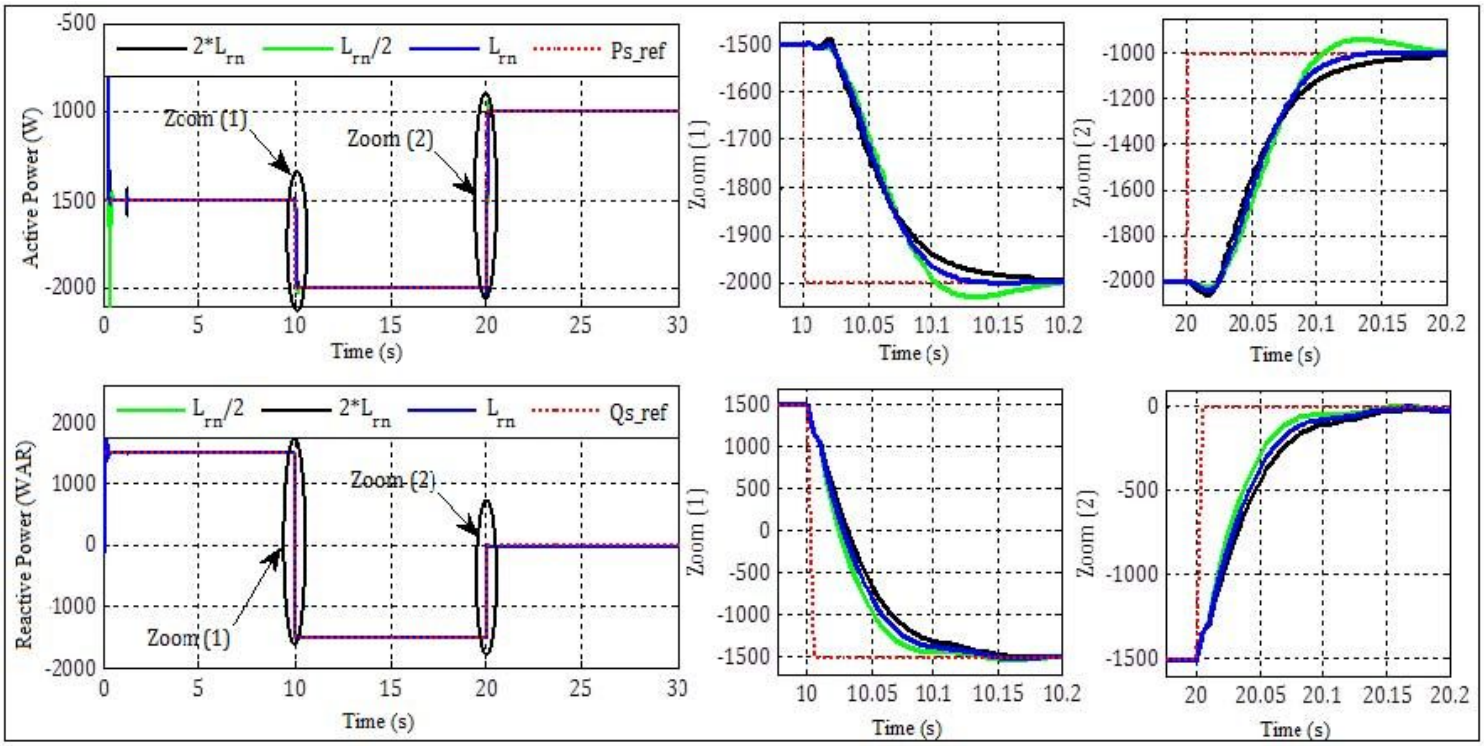

Figure 8

Robustness test during inductance variation

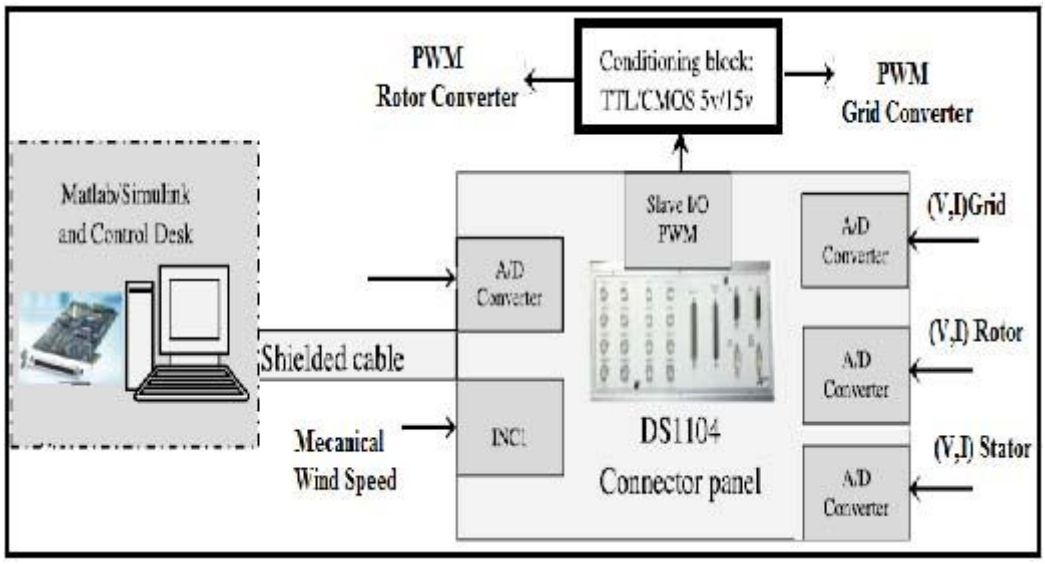

Figure 9

dSPACE connection diagram with the wind system

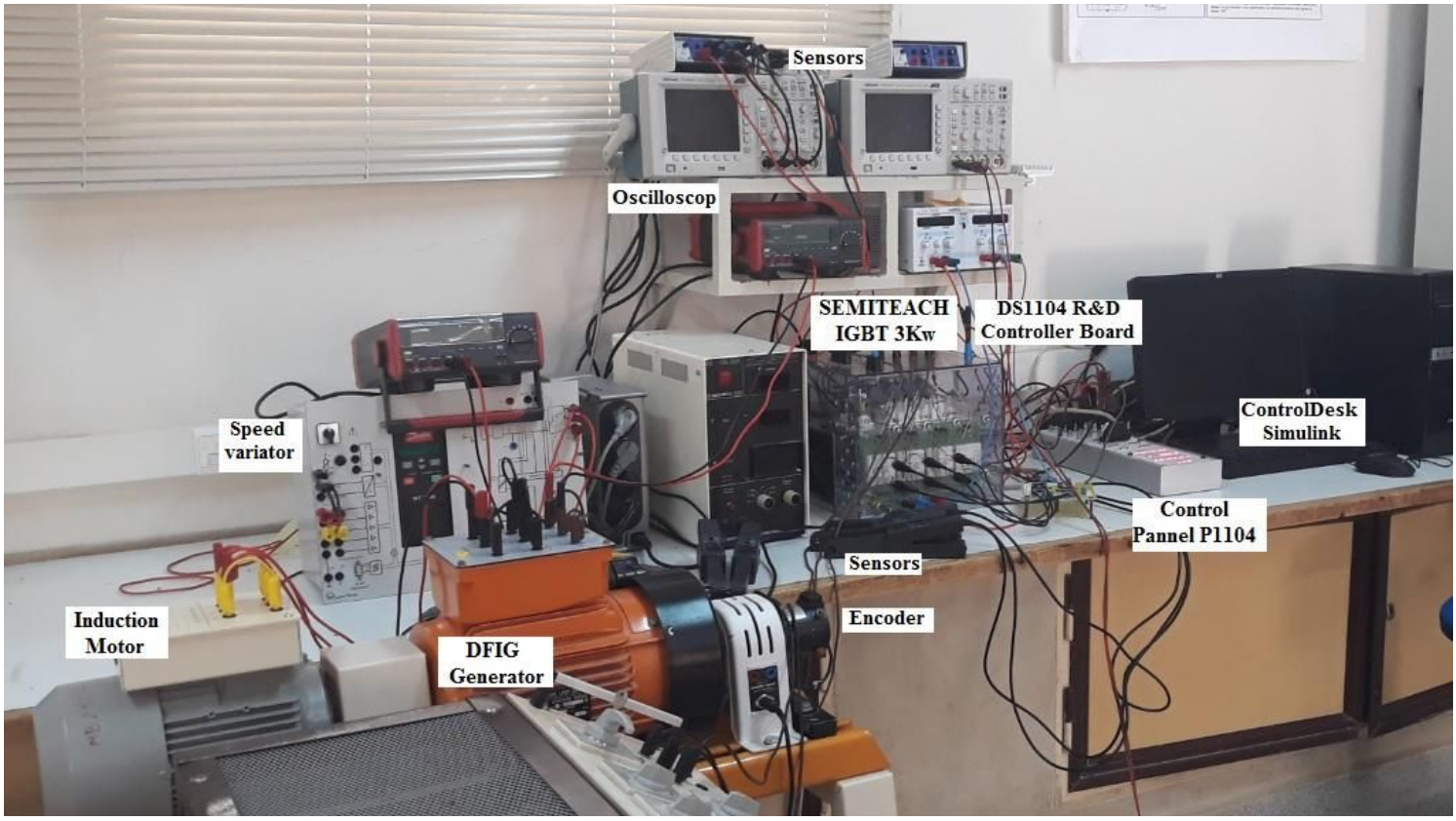

Figure 10

Experimental Benchmark of Wind Turbine System

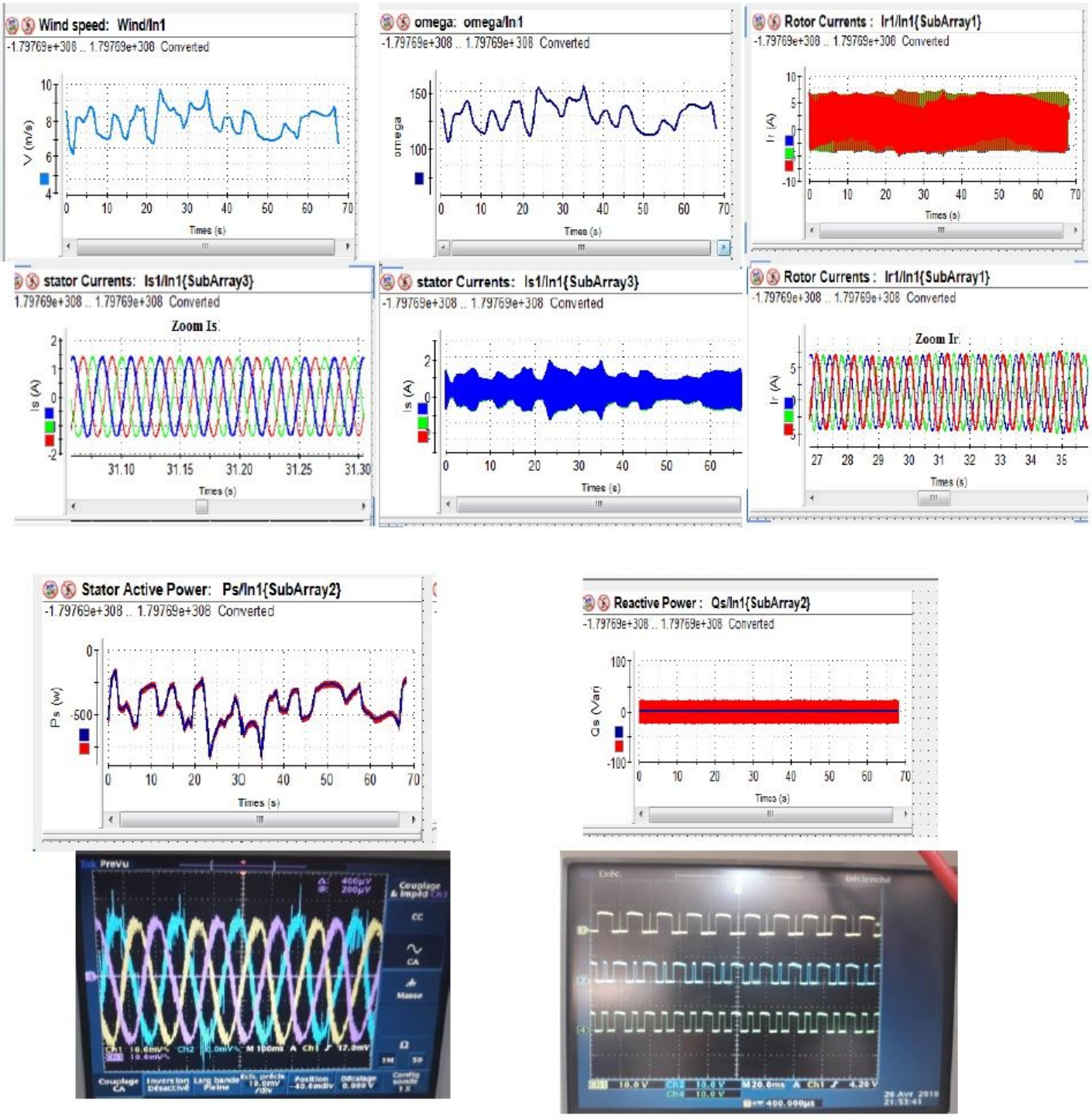

Figure 11

Experimental results of the Backstepping control applied to a WECS